Simulation of the effect of N_2O on DNA damage by ionizing radiation

JIŘÍ BARILLA, PAVEL SIMR, KVĚTUŠE SÝKOROVÁ
Faculty of Science
J. E. Purkinje University in Usti nad Labem
Pasteurova 3544/1, 400 96 Usti nad Labem
CZECH REPUBLIC

Abstract: Damage to the DNA molecule by ionizing radiation can be influenced by the presence of certain chemicals in the cell during irradiation. These substances can be both radioprotective and radiosensitive. In this paper, we will discuss the effect of N_2O, widely used in medicine, on the chemical stage of the radiobiological mechanism. N_2O in the cell during irradiation with ionizing radiation results in more significant damage to the DNA molecule because N_2O reacts with hydrated electrons e_{aq}^- to form aggressive *OH* radicals. A mathematical simulation model developed using hybrid Petri nets is used to analyze this dynamic process. Hybrid Petri nets allow us to quickly create a mathematical simulation model and explore the system under study to obtain detailed information for practical applications.

Key-Words: Hybrid Petri nets, SSB formation, ionizing radiation, radical clusters, N_2O

Received: February 19, 2023. Revised: February 19, 2024. Accepted: May 16, 2024. Published: July 2, 2024.

1 Introduction

When a cell is irradiated with ionizing radiation, energy is absorbed in the medium to form a radical cluster that can damage the DNA molecule. This damage can occur through either direct or indirect effects. A direct effect occurs when the energy transfer from the ionizing radiation occurs near the DNA molecule. This effect is unlikely for low-LET radiation and is neglected in our mathematical simulation model. Much more relevant to us is the damage to the DNA molecule by an indirect effect, where the energy transfer occurs at some distance from the DNA molecule. In our mathematical simulation model, we assume that the damage to the DNA molecule occurs through indirect effects.

Since the cell is primarily composed of water, a radical cluster is formed when the energy of ionizing radiation is transferred to the aqueous environment. Initially (immediately after energy transfer), the radical cluster contains aggressive radicals $H^\bullet, OH^\bullet$ and $HO_2^\bullet$, hydrated electrons e_{aq}^-, and H_3O^+ ions. Immediately after forming the radical cluster, chemical reactions of the chemicals in the cluster occur with simultaneous diffusion of these compounds into the surroundings. If a DNA molecule is close to the radical cluster, the aggressive radicals will react with this molecule to form SSBs (single-strand breaks) and DSBs (double-strand breaks). A necessary condition for the formation of SSBs and DSBs is a sufficient concentration of radicals at the time of the interaction of the cluster with the DNA molecule. For our mathematical simulation model, we will assume low-LET irradiation, which allows us to treat radical cluster diffusion as a spherically symmetric case.

Our mathematical simulation model must include both the dynamics of the chemical reactions of the aggressive radicals and other chemicals present in the radical cluster and the diffusion of these chemicals into the surroundings. If a DNA molecule is close enough to the radical cluster, the DNA molecule will interact with the aggressive radicals (especially the OH radical) to form SSBs and DSBs. The condition is that there is a sufficient concentration of aggressive radicals at the time of the interaction. Therefore, the interaction of the DNA molecule with the radical cluster must occur immediately after forming this cluster in sufficient proximity because the concentration of radicals decreases rapidly due to chemical

reactions and their diffusion into the surroundings.

This process is affected by the presence of N_2O in the cell during irradiation with ionizing radiation so that N_2O molecules react with the hydrated electrons to form aggressive OH radicals that cause more damage to the DNA molecule [1][2]. N_2O thus acts as a radiosensitive substance. In this work, analyses will be performed to show in detail how N_2O affects the chemical stage of the radiobiological mechanism. Hybrid Petri nets proved to be a suitable tool to simulate the dynamic process of DNA molecule damage by aggressive radicals in the presence of N_2O during irradiation with ionizing radiation. These Petri nets allow the rapid generation of a mathematical simulation model using a graphical tool and quick analysis under different input conditions.

We have many years of experience building mathematical simulation models of the chemical stage of the radiobiological mechanism. Initially, we used the Fortran programming language to construct mathematical simulation models [3][4] and later Petri nets, which allowed us to build mathematical simulation models much faster using a graphical tool. Similarly, the analysis of the system under study was much faster [5][6][7][8][9]. Our simulation model contains a minimal number of free parameters, which provides greater model plausibility. The initial model parameters are mostly taken from the literature [10][12][13][14][18][19][21][22][23][24][25][31] [32] and from our previous analyses based on experimental data.

2 Simulation model of DNA damage by ionizing radiation in the presence of N_2O

As mentioned earlier, when cells are irradiated with ionizing radiation, energy is transferred to the aqueous environment to form a radical cluster, which initially contains primary products $(e_{aq}^{-}, H^{\bullet}, OH^{\bullet}, H_3O^{+}, H_2)$ and associated products $(OH^{-}, H_2O_2, O_2^{-}, HO_2^{\bullet})$ formed by subsequent chemical reactions. The mathematical simulation model is intended to describe the dynamics of chemical reactions with the simultaneous diffusion of chemicals into the cluster surroundings. Hybrid Petri nets are a very suitable tool for the development of the simulation model, as they allow easy creation of the mathematical simulation model and its analysis [16][17][27][28][29] [30] [33]. We used the Visual Object Net++ tool [26] to build our mathematical simulation model, which allows the use of hybrid Petri nets and is very easy to work with.

A detailed derivation of the mathematical simulation model has been performed in our previous works [5][6][7][8][9]. In this work, we will only present an extension of the mathematical simulation model to include the interaction of the DNA molecule with aggressive radicals to form SSBs and DSBs. The effect of N_2O during irradiation with ionizing radiation is also included. N_2O affects the chemical stage of the radiobiological mechanism by acting as a radiosensitive substance, causing more damage to the DNA molecule so that N_2O reacts with the hydrated electron according to the reaction

$$e_{aq}^{-} + N_2O \rightarrow N_2 + OH^{-} + OH^{\bullet}$$

This chemical reaction produces additional aggressive OH radicals, which are the primary cause of damage to the DNA molecule.

The whole process of the chemical stage of the radiobiological mechanism can be described as follows: after the transfer of the energy of the ionizing radiation to the aqueous environment, a radical cluster is formed, which initially contains only the primary products of water radiolysis $(e_{aq}^{-}, H^{\bullet}, OH^{\bullet}, H_3O^{+}, H_2)$, whose quantity is determined by the initial yield G^0 corresponding to the transferred energy. Immediately after forming the radical cluster, the primary products of radiolysis begin to react with each other and other molecules present in the radical cluster, according to Table 1.

Table 1. Recombination reactions [14][15][22]

Reaction			Rate constants ($dm^3.mole^{-1}.s^{-1}$)
1.	$H^\bullet + H^\bullet \rightarrow$	H_2	10×10^{10}
2.	$e_{aq}^- + H^\bullet \rightarrow$	$H_2 + OH^-$	2.5×10^{10}
3.	$e_{aq}^- + e_{aq}^- \rightarrow$	$H_2 + 2OH^-$	6×10^9
4.	$e_{aq}^- + OH^\bullet \rightarrow$	$OH^- + H_2O$	3×10^{10}
5.	$H^\bullet + OH^\bullet \rightarrow$	H_2O	2.4×10^{10}
6.	$OH^\bullet + OH^\bullet \rightarrow$	H_2O_2	4×10^9
7.	$H_3O^+ + e_{aq}^- \rightarrow$	$H^\bullet + H_2O$	2.3×10^{10}
8.	$HO_2^\bullet + H^\bullet \rightarrow$	H_2O_2	1×10^{10}
9.	$HO_2^\bullet + OH^\bullet \rightarrow$	$H_2O + O_2$	1×10^{10}
10.	$HO_2^\bullet + HO_2^\bullet \rightarrow$	$H_2O_2 + O_2$	2×10^6
11.	$O_2^- + H_3O^+ \rightarrow$	$HO_2^\bullet$	3×10^{10}
12.	$H_3O^+ + OH^- \rightarrow$	H_2O	1×10^{11}
13.	$H^\bullet + H_2O_2 \rightarrow$	$H_2O + OH^\bullet$	1×10^8
14.	$e_{aq}^- + H_2O_2 \rightarrow$	$OH^\bullet + OH^-$	1.2×10^{10}
15.	$OH^\bullet + H_2O_2 \rightarrow$	$H_2O + HO_2^\bullet$	5×10^7
16.	$OH^\bullet + H_2 \rightarrow$	$H_2O + H^\bullet$	6×10^7
17.	$HO_2^\bullet \rightarrow$	$H_3O^+ + O_2^-$	1×10^6
18.	$e_{aq}^- + O_2 \rightarrow$	$O_2^- + H_2O$	1.9×10^{10}
19.	$H^\bullet + O_2 \rightarrow$	$HO_2^\bullet$	1×10^{10}
20.	$DNA + H^\bullet \rightarrow$	SSB	2.0×10^7
21.	$DNA + OH^\bullet \rightarrow$	SSB	4.0×10^8
22.	$DNA + e_{aq}^- \rightarrow$	SSB	1.5×10^8
23.	$DNA + HO_2^\bullet \rightarrow$	SSB	2.48×10^8
24.	$e_{aq}^- + N_2O \rightarrow$	$N_2 + OH^- + OH^\bullet$	9.1×10^9

Simultaneously with the chemical reactions, primary radiolysis products and newly formed chemicals diffusion into the cluster surroundings. Both result in a decrease in these chemicals. The diffusion rate is then determined by the diffusion coefficients listed in Table 2.

Table 2. Diffusion coefficients [19]

Substance		Diffusion coefficient ($nm^2.ns^{-1}$)	Species amount	Designation of diff. coefficients
1.	$H^\bullet$	7.0	N_H	D_H
2.	$OH^\bullet$	2.2	N_{OH}	D_{OH}
3.	e_{aq}^-	4.9	N_e	D_e
4.	H_3O^+	9.5	$N_{H_3O^+}$	$D_{H_3O^+}$
5.	OH^-	5.3	N_{OH^-}	D_{OH^-}
6.	H_2	5	N_{H_2}	D_{H_2}
7.	H_2O_2	2.2	$N_{H_2O_2}$	$D_{H_2O_2}$
8.	O_2^-	1.8	$N_{O_2^-}$	$D_{O_2^-}$
9.	$HO_2^\bullet$	2.3	N_{HO_2}	D_{HO_2}

Hybrid Petri nets were used to simulate the chemical stage of the radiobiological mechanism, which includes both the dynamics of the chemical reactions according to Table 1, including the diffusion of chemicals into the surroundings of the radical cluster and the interaction of aggressive radicals with the DNA molecule. The mathematical simulation model was created using the graphical tool Visual Object Net++ [26], which allows the creation of discrete and continuous models. A graphical representation of the mathematical simulation model is shown in Figure 1.

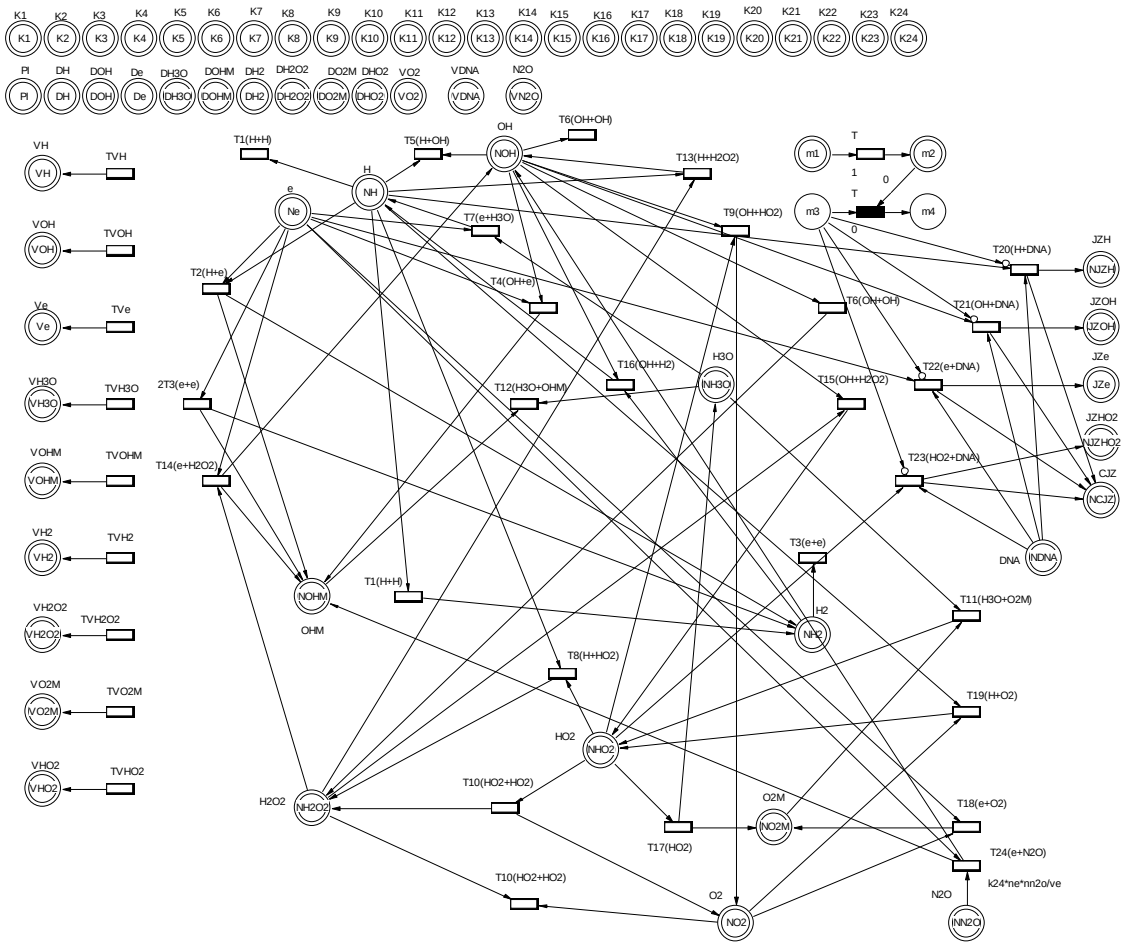

Figure 1. Simulation model of SSB formation represented by hybrid Petri nets.

In Figure 1, we see circles and rectangles connected by arrows. The circles indicate the places that represent the chemical amounts, the size of the volume in which the chemical is found, and the constants used in the mathematical model. The rectangles represent the transitions that cause a change in the value of the location to which arrows connect them. Only the place with the transition can be linked. You cannot connect two places or two transitions.

The circles (places) at the top of Figure 1 represent constants because they are not connected to any rectangle (transition), so their value does not change. They are the rate constants from Table 1, the diffusion coefficients from Table 2, and others.

The locations on the left in Figure 1 represent the volumes in which each chemical in Table 2 is found. Arrows connect these locations to the corresponding transitions that cause the volume value to change. The magnitude of this change depends on the transition function associated with the transition and the direction of the arrow. Assuming the transition function is positive, and the arrow points to a place, the volume value will increase, corresponding to a diffusion process. The places and transitions are labeled to identify the chemical to which they belong. The place designations VH, VOH, Ve, VH3O, VOHM,

VH2, VH2O2, VOHM, and VHO2 correspond to the volumes V_H, V_{OH}, V_e, $V_{H_3O^+}$,V_{OH^-}, V_{H_2}, $V_{H_2O_2}$, $V_{O_2^-}$ and V_{HO_2}, where the subscript indicates the chemical. The corresponding transitions that cause a volume change at the corresponding location are then named TVH, TVOH, TVe, TVH3O, TVOHM, TVH2, TVH2O2, TVOHM, and TVHO2. These are also the names of the transition functions. These transitions are in the form.

$$TVH = 128\sqrt{\left(\frac{D_H^3 t}{\pi}\right)}, \quad (1)$$

$$TVOH = 128\sqrt{\left(\frac{D_{OH}^3 t}{\pi}\right)}, \quad (2)$$

$$TVe = 128\sqrt{\left(\frac{D_e^3 t}{\pi}\right)}, \quad (3)$$

$$TVH3O = 128\sqrt{\left(\frac{D_{H_3O^+}^3 t}{\pi}\right)}, \quad (4)$$

$$TVOHM = 128\sqrt{\left(\frac{D_{OH^-}^3 t}{\pi}\right)}, \quad (5)$$

$$TVH2 = 128\sqrt{\left(\frac{D_{H_2}^3 t}{\pi}\right)}, \quad (6)$$

$$TVH2O2 = 128\sqrt{\left(\frac{D_{H_2O_2}^3 t}{\pi}\right)}, \quad (7)$$

$$TVO2M = 128\sqrt{\left(\frac{D_{O_2^-}^3 t}{\pi}\right)}, \quad (8)$$

$$TVHO2 = 128\sqrt{\left(\frac{D_{HO_2}^3 t}{\pi}\right)}, \quad (9)$$

where D_H, D_{OH}, D_e, $D_{H_3O^+}$, D_{OH^-}, D_{H_2}, $D_{H_2O_2}$, $D_{O_2^-}$ and D_{HO_2} are diffusion coefficients from Table 2.

The mathematical derivation of the transition functions has been done in our previous work [5][6][7][8][9]. The derivation of these mathematical relations assumes spherical symmetry in the diffusion of the radical cluster.

The dynamics of the chemical stage of the radiobiological mechanism can then be simulated by the places and transitions located in the middle of Figure 1 and on its right side. Each place represents the amount of chemical substance changed by the transitions connected to that place. Each place is labeled so that outside the circle is the name of the chemical corresponding to that place, and inside the circle is the name of the variable used in the corresponding transition function. The names H, OH, e, H_3O^+, OH^-, H_2, H_2O_2, O_2^-, HO_2, O_2, and N_2O are used to denote the chemicals H, OH, e, H3O, OHM, H2, H2O2, O2M, HO2, O2, and N2O, respectively. The corresponding variable names are NH, NOH, Ne, NH3O, NOHM, NH2, NH2O2, NO2M, NHO2, NO2, and NN2O. These variables determine the number of particles of each chemical at a given place. The change of the values of the individual places and, thus, the dynamics of the chemical reactions listed in Table 1 are provided by transitions using transition functions of the form:

$$T_1(H+H) = k_1 \frac{N_H(t)N_H(t)}{V_H(t)}, \quad (10)$$

$$T_2(H+e) = k_2 \frac{N_H(t)N_e(t)}{V_H(t)}, \quad (11)$$

$$T_3(e+e) = k_3 \frac{N_e(t)N_e(t)}{V_e(t)}, \quad (12)$$

$$T_4(OH+e) = k_4 \frac{N_{OH}(t)N_e(t)}{V_e(t)}, \quad (13)$$

$$T_5(H+OH) = k_5 \frac{N_H(t)N_{OH}(t)}{V_H(t)}, \quad (14)$$

$$T_6(OH+OH) = k_6 \frac{N_{OH}(t)N_{OH}(t)}{V_{OH}(t)}, \quad (15)$$

$$T_7(e+H3O) = k_7 \frac{N_e(t)N_{H_3O^+}(t)}{V_{H_3O^+}(t)}, \quad (16)$$

$$T_8(H + HO2) = k_8 \frac{N_H(t)N_{HO_2}(t)}{V_H(t)}, \quad (17)$$

$$T_9(OH + HO2) = k_9 \frac{N_{OH}(t)N_{HO_2}(t)}{V_{HO_2}(t)}, \quad (18)$$

$$T_{10}(HO2 + HO2) = k_{10} \frac{N_{HO_2}(t)N_{HO_2}(t)}{V_{HO_2}(t)}, \quad (19)$$

$$T_{11}(H3O + O2M) = k_{11} \frac{N_{H_3O^+}(t)N_{O_2^-}(t)}{V_{H_3O^+}(t)}, \quad (20)$$

$$T_{12}(H3O + OHM) = k_{12} \frac{N_{H_3O^+}(t)N_{OH^-}(t)}{V_{H_3O^+}(t)}, \quad (21)$$

$$T_{13}(H + H2O2) = k_{13} \frac{N_H(t)N_{H_2O_2}(t)}{V_H(t)}, \quad (22)$$

$$T_{14}(e + H2O2) = k_{14} \frac{N_e(t)N_{H_2O_2}(t)}{V_e(t)}, \quad (23)$$

$$T_{15}(OH + H2O2) = k_{15} \frac{N_{OH}(t)N_{H_2O_2}(t)}{V_{H_2O_2}(t)}, \quad (24)$$

$$T_{16}(OH + H2) = k_{16} \frac{N_{OH}(t)N_{H_2}(t)}{V_{H_2}(t)}, \quad (25)$$

$$T_{17}(HO2) = k_{17}N_{(HO_2)}(t), \quad (26)$$

$$T_{18}(e + O2) = k_{18} \frac{N_e(t)N_{O_2}(t)}{V_e(t)}, \quad (27)$$

$$T_{19}(H + O2) = k_{19} \frac{N_H(t)N_{O_2}(t)}{V_H(t)}. \quad (28)$$

$$T_{20}(PDNA + H) = k_{20} \frac{N_{PDNA}(t)N_H(t)}{V_H(t)}. \quad (29)$$

$$T_{21}(PDNA + OH) = k_{21} \frac{N_{PDNA}(t)N_{OH}(t)}{V_{OH}(t)}. \quad (30)$$

$$T_{22}(PDNA + e) = k_{22} \frac{N_{PDNA}(t)N_e(t)}{V_e(t)}. \quad (31)$$

$$T_{23}(PDNA + HO2) = k_{23} \frac{N_{PDNA}(t)N_{HO_2}(t)}{V_{HO_2}(t)}. \quad (32)$$

$$T_{24}(e + N2O) = k_{24} \frac{N_e(t)N_{N_2O}(t)}{V_e(t)}. \quad (33)$$

The mathematical derivation of these transition functions has also been done in our previous work [5][6][7][8][9]. The indices for the symbol T indicate the reaction number in Table 1, and the chemicals that react together are listed in parentheses after the index. To the right of the equation is the corresponding mathematical expression. For example, the math equation

$$T_5(H + OH) = k_5 \frac{N_H(t)N_{OH}(t)}{V_H(t)}$$

the *H* and *OH* radicals react together according to Equation 5 in Table 1. The rate constant k_5 and the mathematical expression behind the rate constant give the rate of this chemical reaction. N_H and N_{OH} are the number of *H*-radical particles, and *OH* and *VH* are the volumes in which the *H*-radical is located. Such labeled transitions can be found in Figure 1. If the arrows point from the places to the corresponding transition, these substances are lost due to chemical reactions. On the other hand, if the arrows point from the transition to the places, new chemicals are being formed, and the values at those places are increasing. These logical connections between places and transitions correspond to the chemical reactions in Table 1.

In the upper right part of Figure 1, there is a part that ensures the delay of the interaction of the DNA molecule with aggressive radicals using a test edge and inhibitors. This makes it possible to simulate the interaction of a DNA molecule with aggressive radicals at different distances of this molecule from the radical cluster.

The mathematical simulation model in Figure 1 describes a system of ordinary differential equations solving dynamics of chemical reactions from Table 1 and the diffusion of the newly arising chemicals into their surroundings. Time dependences of the individual chemicals can then be expressed for better clarity by the following system of ordinary differential equations:

$$\frac{dN_H}{dt} = -2T_{1(H+H)} - T_2(H+e) - T_5(H+OH) - T_8(H+HO2) - T_{13}(H+H2O2)$$
$$-T_{19}(H+O2) - T_{20}(PDNA+H) + T_7(e+H3O) + T_{16}(OH+H2) \quad (34)$$

$$\frac{dN_{OH}}{dt} = -T_4(OH+e) - T_5(H+OH) - 2T_6(OH+OH) - T_9(OH+HO2)$$
$$-T_{15}(OH+H2O2) - T_{16}(OH+H2) - T_{21}(PDNA+OH) + T_{13}(H+H2O2)$$
$$+T_{14}(e+H2O2) + T_{24}(e+N2O) \quad (35)$$

$$\frac{dN_e}{dt} = -T_2(H+e) - 2T_3(e+e) - T_4(OH+e) - T_7(e+H3O) - T_{14}(e+H2O2)$$
$$-T_{18}(e+O2) - T_{22}(PDNA+e) - T_{24}(e+N2O) \quad (36)$$

$$\frac{dN_{H_3O^+}}{dt} = -T_7(e+H3O) - T_{11}(H3O+O2M) - T_{12}(H3O+OHM) + T_{17}(HO2) \quad (37)$$

$$\frac{dN_{OH^-}}{dt} = -T_{12}(H3O+OHM) + T_2(H+e) + 2T_3(e+e) + T_4(OH+e) + T_{14}(e+H2O2)$$
$$+T_{24}(e+N2O) \quad (38)$$

$$\frac{dN_{H_2}}{dt} = -T_{16}(OH+H2) + T_1(H+H) + T_2(H+e) + T_3(e+e) \quad (39)$$

$$\frac{dN_{H_2O_2}}{dt} = -T_{13}(H+H2O2) - T_{14}(e+H2O2) - T_{15}(OH+H2O2) + T_6(OH+OH)$$
$$+T_8(H+HO2) + T_{10}(HO2+HO2) \quad (40)$$

$$\frac{dN_{O_2^-}}{dt} = -T_{11}(H3O+O2M) + T_{17}(HO2) + T_{18}(e+O2) \quad (41)$$

$$\frac{dN_{HO_2}}{dt} = -T_8(H+HO2) - T_9(OH+HO2) - 2T_{10}(HO2+HO2) - T_{17}(HO2)$$
$$-T_{23}(PDNA+HO2) + T_{11}(H3O+O2M) + T_{15}(OH+H2O2) + T_{19}(H+O2) \quad (42)$$

$$\frac{dN_{O_2}}{dt} = -T_{18}(e+O2) - T_{19}(H+O2) + T_9(OH+HO2) + T_{10}(HO2+HO2) \quad (43)$$

$$\frac{dN_{NDNA}}{dt} = -T_{20}(NDNA+H) - T_{21}(NDNA+OH) - T_{22}(NDNA+e) - T_{23}(NDNA+HO2) \quad (44)$$

$$\frac{dN_{N_2O}}{dt} = -T_{24}(e+N2O) \quad (45)$$

where N_H, N_{OH}, N_e, $N_{H_3O^+}$, N_{OH^-}, N_{H_2}, $N_{H_2O_2}$, $N_{O_2^-}$, N_{HO_2}, N_{O_2} and N_{NDNA} represent numbers of species H, OH, e, H_3O^+, OH^-, H_2, H_2O_2, O_2^-, HO_2, O_2 and *DNA* (number of phosphate bonds) respectively, which are placed in corresponding volumes V_H, V_{OH}, V_e, $V_{H_3O^+}$, V_{OH^-}, V_{H_2}, $V_{H_2O_2}$, $V_{O_2^-}$, V_{HO_2}, V_{O_2} and V_{DNA}. k_1, k_2, …, k_{24} are rate constants of the chemical reactions from Table 1.

Immediately after the energy transfer to the radical cluster, the radicals diffuse into the surroundings, and the volumes V_H, V_{OH}, V_e, $V_{H_3O^+}$, V_{OH^-}, V_{H_2}, $V_{H_2O_2}$, $V_{O_2^-}$, and V_{HO_2} increase according to the system of ordinary differential equations.

The system of ordinary differential equations (34-54) describes the same problem as the mathematical simulation model shown in Figure 1 and contains the same transition functions (1-33).

$$\frac{dV_H}{dt} = TVH, \quad (46)$$

$$\frac{dV_{OH}}{dt} = TVOH, \quad (47)$$

$$\frac{dV_e}{dt} = TVe, \quad (48)$$

$$\frac{dV_{H_3O^+}}{dt} = TVH3O, \quad (49)$$

$$\frac{dV_{OH^-}}{dt} = TVOHM, \quad (50)$$

$$\frac{dV_{H_2}}{dt} = TVH2, \quad (51)$$

$$\frac{dV_{H_2O_2}}{dt} = TVH2O2, \quad (52)$$

$$\frac{dV_{O_2^-}}{dt} = TVO2M, \quad (53)$$

$$\frac{dV_{HO_2}}{dt} = TVHO2, \quad (54)$$

3 Application of the mathematical simulation model to specific conditions

For the practical use of our mathematical simulation model, it is necessary to apply it to specific conditions, related in particular to the types of ionizing radiation used, the amount of energy transferred to the aqueous environment, the initial yield of primary radiolysis products, the size of the resulting cluster, and so on. The input parameters of the mathematical simulation model were set based on the analysis of experimental data published in Blok and Loman [11]. These analyses were carried out in our previous work [3][4] and allowed us to set the basic parameters of the model. In the experiment described in the literature by Block and Loman, an aqueous DNA solution was irradiated with Co-60 ionizing radiation.

As mentioned above, a radical cluster is formed immediately after transferring energy to the aqueous environment. Based on the analyses in our previous work, the amount of energy transferred to the radical cluster was 300 eV, and the corresponding radical cluster diameter was 27 nm. The radical cluster initially contains the following chemicals: $H^\bullet$, $OH^\bullet$, e_{aq}^-, H_3O^+, and H_2. Their initial amounts of N_H, N_{OH}, N_e, $N_{H_3O^+}$, and N_{H_2} are given by the radiolysis yield

of water G^0 under anoxic conditions [14][18][19][20][23].

For a cluster with a diameter of 27 nm and a transition energy of 300 eV, the following initial chemical numbers were determined

$$N_{H^\bullet} = 1.26,\ N_{OH^\bullet} = 16.5,\ N_e = 14.34,\ N_{H_3O^+} = 14.34,\ N_{H_2} = 0.45,$$

These initial chemicals then give rise to other chemicals according to the reactions shown in Table 1, where the reaction constants of these chemical reactions are also given. The dynamic process then proceeds according to the transition functions (10-33), where the rate constants $k_1 - k_{24}$ (see Table 1) are taken from the literature.

Simultaneously with the chemical reactions in the radical cluster, the newly formed chemical species diffuse into the surroundings. In our work, we assume spherical symmetry for the time evolution of the radical cluster, which corresponds to low-LET radiation. The diffusion coefficients are then listed in Table 2 and taken from the literature. The time evolution of the radical cluster for the chemicals in Table 2 follows transition functions 1-9.

The interaction of the DNA molecule with aggressive radicals results in the formation of SSBs and DSBs, which cause DNA damage. This damage occurs only if the DNA molecule is close enough to the radical cluster and the concentration of aggressive radicals is high enough at the interaction time. The *OH* radical is a significant contributor to DNA damage.

To verify the correctness of our mathematical simulation model, the experimental data of Blok and Loman were used in our previous analyses [3][4]. Using our mathematical simulation model, we obtained a value of 4 SSBs for the zero N_2O concentration under normal conditions and a value of 6 SSBs for the saturated N_2O solution (see Figure 2), which agrees with the experimental data.

Figure 2 shows the dependence of the number of SSBs on the N_2O concentration under normal conditions. The support of the total number of SSBs formed and the number of SSBs on the *H* and *OH* radicals, the hydrated electron e_{aq}^- and the HO_2 ion are shown. Figure 2 shows that the *OH* radical has the most significant effect on damaging the DNA molecule and that the impact of other chemicals is negligible. We can also see that as the concentration of N_2O increases, the number of SSBs increases, resulting in more damage to the DNA molecule. The increase in the number of *OH* radicals occurs in the presence of N_2O, according to reaction 24 in Table 1. This can be used wherever we need to increase the effect of ionizing radiation on a cell at the same dose. In radiotherapy, we achieve more significant damage to tumor cells, just as in food irradiation, we can better destroy unwanted bacteria. Wastewater treatment and radiosterilisation can also take advantage of this effect. Our analysis in Figure 2 allows us to estimate the number of SSBs at different N_2O concentrations, which is helpful for practical applications.

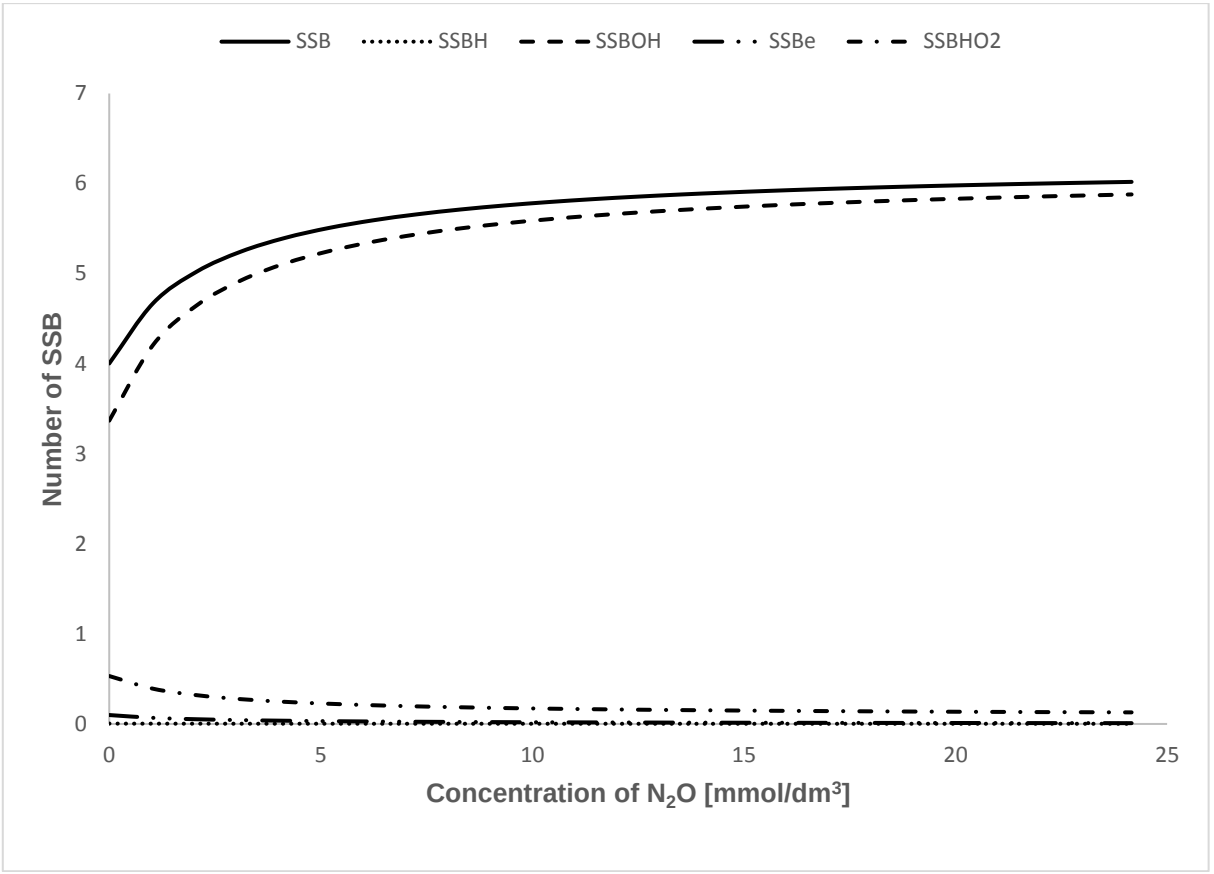

Figure 2. Dependence of the number of SSBs on the N_2O concentration under normal conditions.

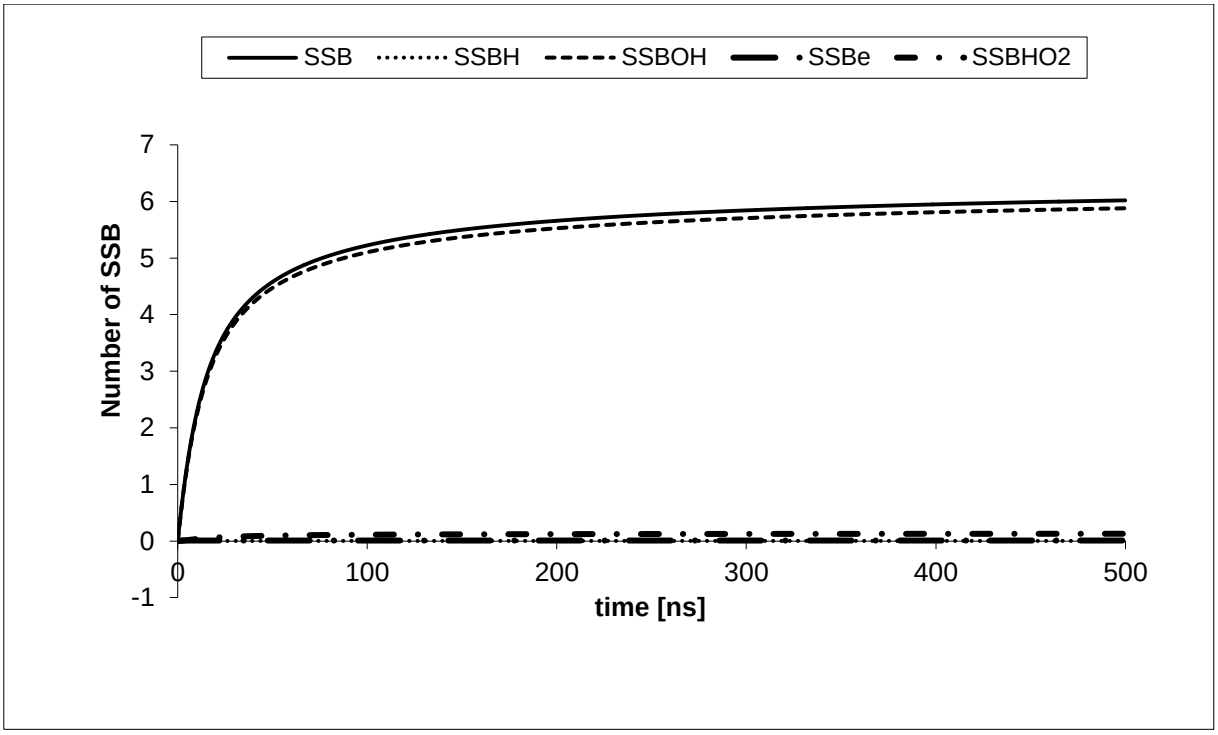

Figure 3. Time dependence of the number of SSBs under normal conditions.

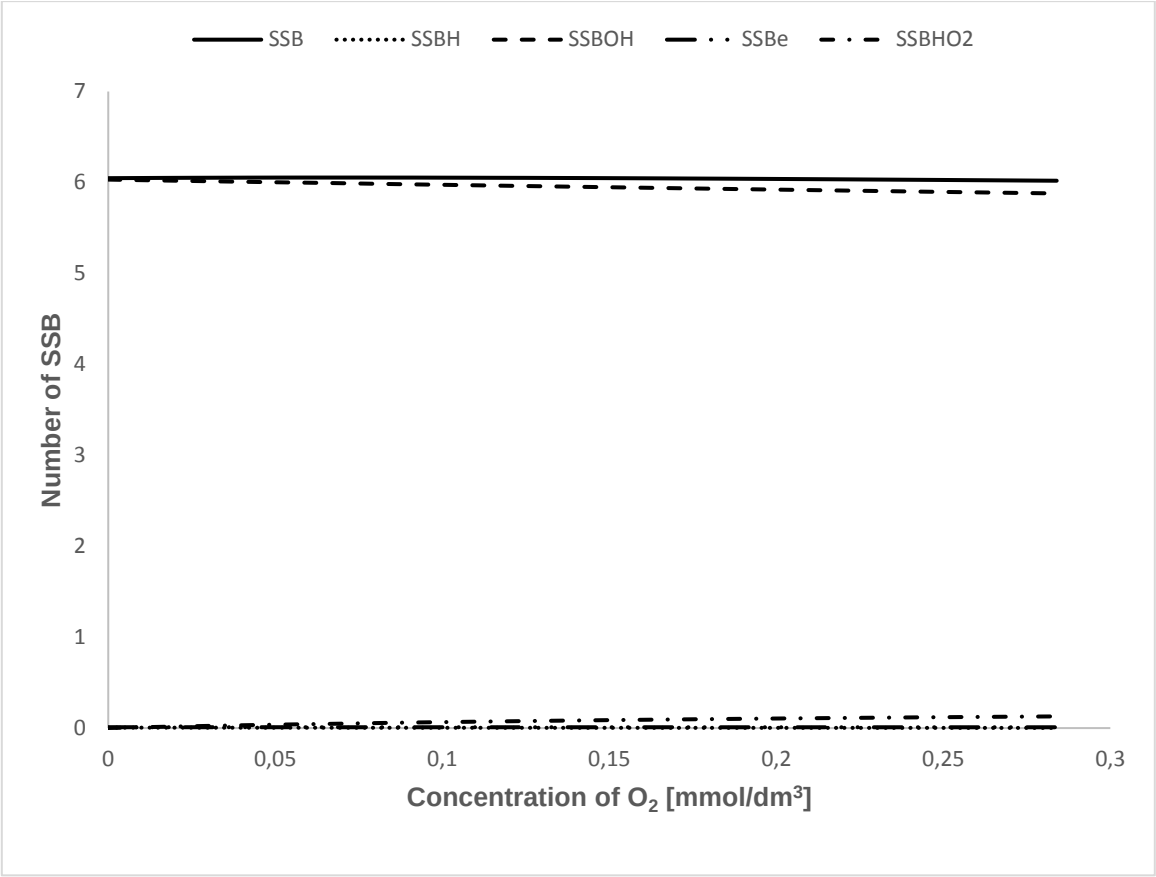

Figure 4. Dependence of the number of SSBs on the O_2 concentration at saturated N_2O.

The time dependence of the number of SSBs is shown in Figure 3. Initially, there is a sharp increase in SSBs, then the growth slows down. This is because, at the beginning of the interaction of the DNA molecule with the radical cluster, the concentration of radicals is highest and then gradually decreases due to chemical reactions and diffusion of aggressive chemicals into the environment. Again, we see that the *OH* radical has a much higher concentration than the other chemicals that cause SSBs on the DNA molecule all the time. From Figure 3, we can conclude that most SSBs enter in a short time after the formation of the radical cluster. This is due to a sharp decrease in the concentration of aggressive radicals caused by chemical reactions and diffusion of the radical into the surroundings.

Figure 4 shows an interesting analysis of the effect of oxygen concentration at saturated N_2O. Based on this analysis, we found that the oxygen concentration had little effect on the number of SSBs formed. There was a slight decrease in the total number of SSBs from a value of 6.047 to a value of 6.012, which is negligible. The finding that oxygen concentration hardly affects the effect of ionizing radiation on the cell when the N_2O solution is saturated is also essential for practical applications.

For the formation of SSBs, the radical cluster must be formed close enough to the DNA molecule when the radical cluster is not yet too large, and the concentration of aggressive radicals is high enough. The dependence of the number of SSBs formed on the diameter of the radical cluster is then shown in Figure 5. It can be seen that the number of SSBs formed decreases with increasing radical cluster diameter due to diffusion. Initially rapidly and then gradually. Based on this analysis, the degree of DNA damage can be estimated as a function of the distance of the formed radical cluster from the DNA molecule. Based on Figure 5, we can see what damage to the DNA molecule is caused by ionizing radiation when a radical cluster is formed at some distance from the DNA molecule, which is relevant for practical applications.

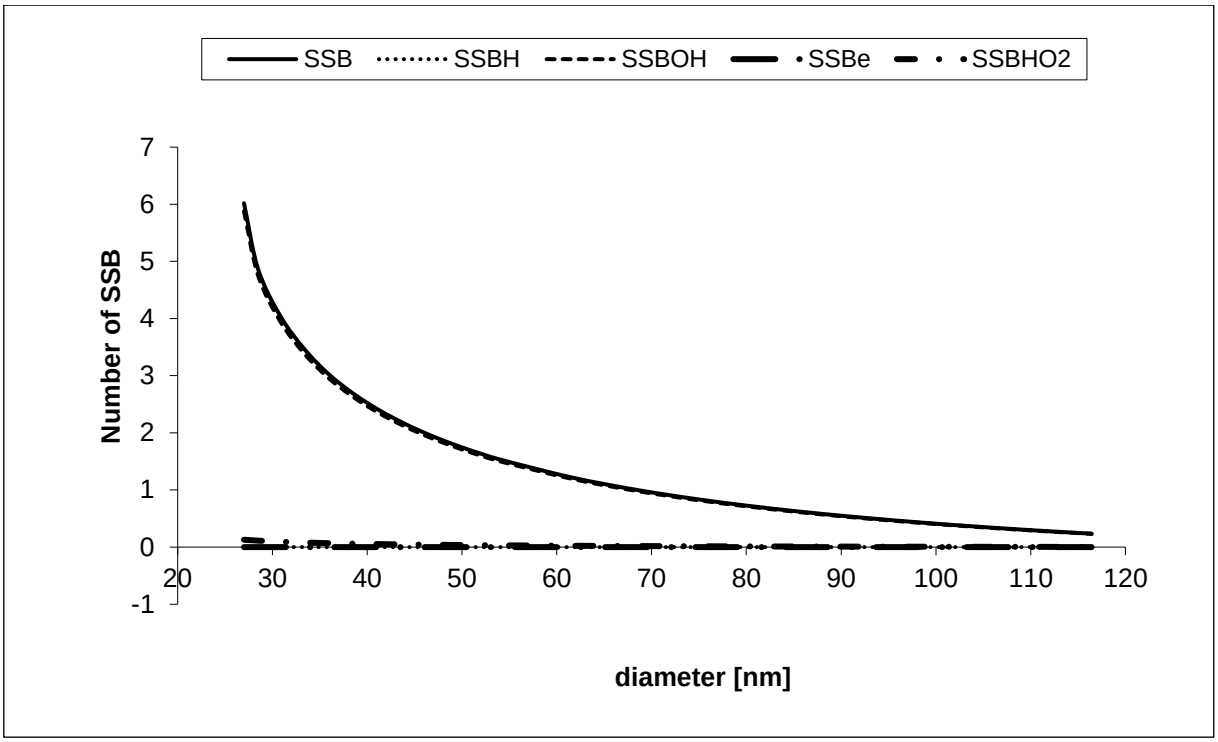

Figure 5. Dependence of the number of SSBs on the cluster diameter at the time of the beginning of the interaction of the DNA molecule with the radical cluster.

Hybrid Petri nets have proven to be a suitable tool for developing a mathematical simulation model to simulate the chemical stage of the radiobiological mechanism. The results obtained with our mathematical simulation model have been validated with experimental data and agree with them. The generally accepted view showed that the *OH* radical is mainly responsible for forming SSBs on the DNA molecule. Another significant fact is that the presence of N_2O in cells causes more damage to the DNA molecule. As mentioned, this fact can be used in radiotherapy, food irradiation, radio sterilization, wastewater irradiation, and wherever we need to increase the effect of ionizing radiation on the cell. With the same radiation dose, a more significant effect of ionizing radiation on damaging the DNA molecule can be achieved. Another interesting finding is that when N_2O is present in the cell, the oxygen concentration hardly affects the effect of ionizing radiation on the DNA molecule. Also interesting are the observed dependencies of the number of SSBs on time and the distance of the formed cluster from the DNA molecule.

Double-strand breaks (DSBs) are critical for permanent damage to the DNA molecule. A double-strand break occurs when the two resulting single-strand breaks (SSBs) are close enough together on opposite strands of the DNA molecule. If we know the probability of SSBs, we can calculate the probability of DSBs using the equation

$$p_D = \frac{1}{2}\ p_S^2\ , \tag{34}$$

where p_S can be approximately expressed as

$$p_S = \sum_j \int_t \alpha_j\ c_j(t).$$

The α_j parameters represent the efficiency of the individual radicals that react with the DNA molecule to form SSBs, and $c_j(t)$ is the concentration of these radicals.

Another way to obtain the number of DSBs based on the correlation between the number of SSBs and the number of DSBs was described in the literature by Blok and Loman [11]. For low-Let radiation, the ratio of DSBs to SSBs is 1:100. This means that the previously mentioned value of 4 SSBs corresponds to 0.04 DSBs and the value of 6 SSBs corresponds to 0.06 DSBs, which is consistent with our previous work [3][4]. In this way, we can easily convert all the obtained SSB values into numbers of DSBs.

4 Conclusion

In this work, a novel approach has been used to analyze the chemical stage of the radiobiological mechanism in the presence of N_2O in the cell: hybrid Petri nets have been used to construct a mathematical simulation model in which discrete and continuous places and transitions are used. This mathematical simulation model allows us to simulate the entire chemical stage of the radiobiological mechanism, from forming the radical cluster to forming SSBs on the DNA molecule. The simulated dynamic process includes the time evolution of the chemical reactions, as shown in Table 1, under simultaneous chemical diffusion based on the diffusion coefficients shown in Table 2.

The process occurs as ionizing radiation transfers energy to the water environment to form a radical cluster containing aggressive radicals and other chemicals. Immediately after forming the radical cluster, the chemical reactions shown in Table 1 occur, and simultaneously, the newly formed chemicals diffuse into the environment. This results in a decrease in the concentration of aggressive radicals and other chemicals. Our mathematical simulation model assumes that low-LET ionizing radiation is used for irradiation. For this type of radiation, we can assume that the time evolution of the cluster diffusion is spherically symmetric. We further believe that the radical cluster is formed at some distance from the DNA molecule, which means that damage to this molecule occurs indirectly by the aggressive radicals created reacting directly with the DNA molecule to form SSBs and DSBs.

The analyses obtained by our mathematical simulation model concerning the effect of N_2O on the chemical stage of the radiobiological mechanism are very interesting. These analyses showed that the presence of N_2O during the irradiation of a cell with ionizing radiation causes more damage to the DNA molecule. The main contributor is the OH radical, formed in the presence of N_2O according to reaction 24 (see Table 1). Furthermore, the analyses showed that oxygen concentration has little effect on the damage to the DNA molecule in the presence of N_2O. Interestingly, the study also gives us the degree of damage to the DNA molecule as a function of the distance of this molecule from the radical cluster formed.

Our mathematical simulation model using hybrid Petri nets shows a new approach to simulating the radiobiological mechanism's chemical phase. Likewise, the analysis performed in this work provides further information that can be used in radiotherapy, food irradiation, radio sterilization, wastewater irradiation, and wherever we need to increase the effect of ionizing radiation on the cell. The model can be easily adapted to the cylindrical symmetry of the time evolution of the cluster, which will allow its application to other types of ionizing radiation.

In our future research, we will use colored Petri nets to create mathematical simulation models, allowing us to make even more detailed and accurate simulation models. We would also like to simulate the repair of damage to the DNA molecule by repair mechanisms.

In addition to the effect of gamma radiation, we also want to study the effect of protons on the radiobiological mechanism. We aim to use colored Petri nets to create a simulation model that will simulate all three phases of the radiobiological mechanism: physical, chemical, and biological. This model can be used for a more detailed study of radiobiological mechanisms and in practice in testing radioprotective and radiosensitive agents.

Acknowledgement:
The Faculty of Science, J. E. Purkinje University in Usti nad Labem, Czech Republic, supported this work.

References:

[1] Alizadeh E., Cloutier P, Hunting D., Sanche L., Soft X-ray and Low Energy Electron Induced Damage to DNA under N2 and O2 Atmospheres. *J. Phys. Chem. B* 2011; 115:4523–4531. DOI: 10.1021/jp200947g

[2] Alizadeh E., Sanchez L., Induction of strand breaks in DNA films by low energy electrons and soft X-ray under nitrous oxide atmosphere. *Radiation Physics and*

Chemistry 2012; 81:33-39. DOI:10.1016/j.radphyschem.2011.09.004

[3] Barilla J., Lokajíček M., The Role of Oxygen in DNA Damage by Ionizing Particles. *Journal of Theoretical Biology* 2000; 207:405-414. DOI:10.1006/jtbi.2000.2188

[4] Barilla J., Lokajíček M., Pisaková H., et al. Analytical model of chemical phase and formation of DSB in chromosomes by ionizing radiation. *Australasian Physical & Engineering Sciences in Medicine* 2013; 36(1):11-17 DOI: 10.1007/s13246-012-0179-4.

[5] Barilla J., Lokajíček M., Pisaková H., et al. 2014. Simulation of the chemical stage in water radiolysis with the help of Continuous Petri nets. *Radiation Physics and Chemistry* 2014; 97:262-269, DOI: 10.1016/j.radphyschem.2013.12.019.

[6] Barilla J, Lokajicek M, Pisaková H, et al. Applying Petri nets to modeling the chemical stage of radiobiological mechanism. *Physics and Chemistry of Solids* 2015; 78:127–136, DOI: 10.1016/j.jpcs.2014.11.016.

[7] Barilla J., Lokajíček, M., Pisakova, H., Simr, P., 2016. Influence of oxygen on the chemical stage of radiobiological mechanism. *Radiation Physics and Chemistry*. 124, 116-123. DOI: 10.1016/j.radphyschem.2016.01.035.

[8] Barilla J., Lokajíček M., Pisakova H., Simr, P.: Using Petri Nets to Model the Chemical Stages of the Radiobiological Mechanism. New York: *Nova Science Publishers*, 2017. ISBN 978-1-53612-896-3.

[9] Barilla, J., Simr, P., Sýkorová K., Simulation of the influence of N2O on the chemical stage of water radiolysis. *WSEAS Transactions on Biology and Biomedicine*, 2022, 19, 47-62. DOI: 10.37394/23208.2022.19.7.

[10] Beuve M., Colliaux A., Dabli D., et al. Statistical effects of dose deposition in track-structure modelling of radiobiology efficiency. *Nuclear Instruments and Methods in Physics Research Section B: Beam Interactions with Materials and Atoms* 2009*;* 267:983-988. DOI:10.1016/j.nimb.2009.02.016

[11] Blok J., Loman H., The effects of γ - radiation in DNA. *Curr Top Radiat Res Q.* 1973; 9:165-245.

[12] Buxton G.V, Swiatla-Wojcik D., Modeling of Radiation Spur Processes in Water at Temperatures up to 300 C. *J. Phys. Chem.* 1995; 99:11464–11471. DOI:10.1021/j100029a026

[13] Buxton G.V., High Temperature Water Radiolysis. *Radiation Chemistry* 2001; 145-162, ed. Jonah, C. D. and Rao, B. S. M. Elsevier, Amsterdam. DOI:10.1016/S0167-6881(01)80009-4

[14] Buxton G.V., The Radiation Chemistry of Liquid Water. *Charged Particle and Photon Interactions with Matter* 2003; 331-363, ed. Mozumder, A. and Hatano, Y. New York, Marcel Dekker. DOI: 10.1201/9780203913284

[15] Chatterjee A., Maggie J., Dey S., The Role of Homogeneous Reaction in the Radiolysis of Water. *Radiation Research* 1983; 96:1-19. DOI:10.2307/3576159

[16] David R., Alla H., Discrete. *Continuous and Hybrid Petri nets.* Springer-Verlag 2005. DOI:10.1007/b138130

[17] Gu T., Dong R., A novel continuous model to approximate time Petri nets: Modelling and analysis. *Int. J. Appl. Math. Comput. Sci.* 2005; 15:141–150. ISSN: 1641-876X

[18] Hart E. J., Platzman R. L., *Radiation Chemistry*; Academic Press: New York 1961; 93-257, ed. Errera, M. and Forssberg.

[19] Hervé du Penhoat M.A, Goulet T., Frongillo Y., et al. Radiolysis of Liquid Water at Temperatures up to 300oC: Monte Carlo Simulation Study. *J. Phys. Chem.* 2000; 41:11757–11770. DOI:10.1021/jp001662d

[20] Krasilnikov V., Kuplenninov E., Particle Accelerators and Gamma-therapeutic Devices - an Effective Tool for Cancer Treatment. *International Journal on*

Applied Physics and Engineering 2022; 1, 84-94, DOI: 10.37394/232030.2022.1.9

[21] LaVerne J. A, Pimblott S. M., Scavenger and Time Dependences of Radicals and Molecular Products in the Electron Radiolysis of Water. *J. Phys. Chem* 1991; 95:3196–3206. DOI:10.1021/j100161a044

[22] Michaels H.B, Hunt J. V., A model for Radiation Damage in Cells by Direct Effect and by Indirect effect: A Radiation Chemistry Approach. *Radiation Research* 1978; 74: 23-24. DOI:10.2307/3574754

[23] Mozumder A., Magee J. L., Model of Tracks of Ionizing Radiations of Radical Reaction Mechanisms. *Radiation Research* 1966; 28:203–214. DOI: 10.2307/3572190

[24] Mukhomorov V. K., Simulation of the Radioprotective Action of Mercaptoethylamine Derivatives and its Analogues with their Quantum-Chemical and Information Features. *Molecular Science and Applications 2022*; 2, 121-148, DOI: 10.37394/232023.2022.2.14

[25] Pimblott S. M, Mozumder A., Modeling of Physicochemical and Chemical Processes in the Interactions of Fast Charged Particles with Matter, Charged Particle and Photon Interactions with Matter; *Marcel Dekker: New York* 2004; 75-103, ed. Mozumder, A. and Hatano, Y. DOI:10.1201/9780203913284.ch4

[26] Rainer D., Visual Object Net++. Available from: http://www.techfak.uni-bielefeld.de/mchen/ BioPNML/Intro/VON.html. 2008.

[27] Silva M., Recalde L., On fluidification of Petri net models: from discrete to hybrid and continuous models. *Annual Reviews in Control* 2004; 28:253–266. DOI:10.1016/j.arcontrol.2004.05.002

[28] Silva M., Julvez J., Mahulea, C., et al. On fluidization of discrete event models: observation and control of continuous Petri nets. *Discrete Event Dynamic Systems* 2011; 21:4:427-497. DOI:10.1007/s10626-011-0116-9

[29] Staines A. S., Graph Drawing Approaches for Petri Net Models. *WSEAS Transactions on Information Science And Applications* 2020; 17, 110-116, DOI: 10.37394/23209.2020.17.13

[30] Staines A. S., Alternative Matrix Representation of Ordinary Petri Nets. *WSEAS Transactions on Computers* 2019; 18, 11-18, E-ISSN: 2224-2872 11

[31] Uehara S., Nikjoo H., Monte Carlo simulation of water radiolysis for low-energy charged particles. *Journal of Radiation Research* 2006; 47:69–81. DOI:10.1269/jrr.47.69

[32] Watanabe R., Saito K., Monte Carlo simulation of water radiolysis in oxygenated condition for monoenergetic electrons from 100 eV to 1 MeV. *Radiation Physics and Chemistry* 2001; 62:217-228. DOI:10.1016/S0969-806X(01)00195-5

[33] Zacek J., Hunka F., Melis M., Modeling the value chain with object-valued Petri Nets. *Wseas Transactions on Information Science And Applications* 2021; 18, 156-161, DOI: 10.37394/23209.2021.18.19

Contribution of Individual Authors to the Creation of a Scientific Article (Ghostwriting Policy)

The authors equally contributed in the present research, at all stages from the formulation of the problem to the final findings and solution.

Sources of Funding for Research Presented in a Scientific Article or Scientific Article Itself

No funding was received for conducting this study.

Conflict of Interest

The authors have no conflicts of interest to declare that are relevant to the content of this article.